LOGIC
Journal of Engineering Design and Technology
Vol. 26 No. 1 March 2026 ; p. 71 - 78

p-ISSN : 1412-114X
e-ISSN : 2580-5649
http://ojs2.pnb.ac.id/index.php/LOGIC

A NUMERICAL STUDY OF CORRUGATED SIERPINSKI CARPET ON SOLAR DRYER

Lohdy Diana [1)*], Arrad Ghani Safitra [1)], Eli Novita Sari [2)], Firman Yunan Saputra [1)], Ar Rayyan Ikhsan Syahputra[1)], Muhammad Yusuf Febrian Putra [1)], Mutia Ayu Agustina [1)]

1) Power Plant Engineering, Politeknik Elektronika Negeri Surabaya, Jl. Raya ITS, Surabaya, East Java, Indonesia
2) Manufacturing Engineering Technology, Politeknik Negeri Banyuwangi, Banyuwangi, Indonesia

Correponding email [1)*] : lohdydiana@pens.ac.id

Abstract. Solar dryers have problems with low heat transfer performance and uneven temperature distribution, resulting in low efficiency. The efficiency of solar dryers depends on the design of the absorber plate, namely how much it can absorb solar heat. This study applies a Siepinski carpet with a complex structure and large dimensions, resulting in iterations called fractals. This study aims to improve the efficiency of solar dryers as an alternative to the negative impact of falling tomato prices, to determine the effect of the Siepinski Carpet Corrugated fractal distance on the performance of solar dryers in terms of heat transfer, to compare corrugated absorber plates with 3 siepinski carpet corrugated based on variations in the fractal ratio (RF), namely the ratio of the fractal center distance to the fractal length RF = 1, RF = 0.75, and RF = 0.6, on the performance of solar dryers, as well as to determine the distribution of temperature, pressure, and air flow velocity in the collector using the Computational Fluid Dynamics (CFD) simulation method. This study used simulation methods that was conducted in a laboratory. In conclusion, the fractal ratio strongly influences airflow behavior and temperature distribution, where overly dense or overly open configurations enhance heat transfer, while intermediate obstruction can reduce thermal performance. Among the cases studied, RF = 1 and RF = 0.6 provide more effective and consistent heat transfer compared to RF = 0.75.

Keywords : Solar Dryers, Sierpinski Carpet, performance

1. INTRODUCTION

Indonesia is known as an agrarian country with a population that depends on the agricultural sector, supported by a tropical climate and mountains that enrich the soil [1]. The agricultural sector contributes around 13% to the national GDP and will absorb 29% of the workforce by 2022, making it the backbone of the rural economy [BPS 2025 data][2], [3], [4], [5]. However, farmers often suffer losses due to drastic price drops during abundant harvests, as in the cases of Lampung and Bandung where production costs are not covered [6], [7]. This is particularly relevant to Indonesian agriculture, where tomatoes are one of the main commodities with an annual production of 1.2 million tons, but 20-30% are lost post-harvest due to decay and price fluctuations [8][9][10]. Dependence on fresh harvests exacerbates the instability of farmers' incomes, so post-harvest processing such as drying can be a solution to extend shelf life, increase selling value, and support national food security [11].

Conventional sun-based drying is still dominant among Indonesian farmers, but this method is dependent on weather, unhygienic, and difficult to control temperature and humidity, resulting in inconsistent dried product quality. Solar dryers were then developed as an efficient and environmentally friendly solution, utilizing Indonesia's solar radiation potential of 4.8 kWh/m² per day [12]. The performance of dryers is greatly influenced by the design of the heat-absorbing plate, where the application of fractal structures such as Sierpinski Carpet Corrugated (SCC) has been proven to increase efficiency by 32-85% through expanded contact area and more even air flow distribution [13][14][15][16][17].

The Sierpinski Carpet fractal structure is a two-dimensional pattern formed through recursive iteration: starting from a whole square, a square hole is then created in the center (1/9 of the area is lost), and the process is repeated on the sub-squares up to a certain fractal level, resulting in a fractal dimension of approximately 1.89

[18]. This pattern creates a corrugated surface that increases the surface area by 2-3 times compared to a flat plate, facilitating even heat distribution and an optimal laminar-turbulent airflow pattern. Relevant research such as the study by Koch and Löhndorf (2020) on fractal heat exchangers shows a 40% increase in heat transfer thanks to self-similar geometry, while CFD simulations by Wang et al. (2022) on SCC solar air heaters prove 75% thermal efficiency at a fractal ratio of 0.6. The advantages of the Sierpinski Carpet structure include: large surface area for optimal convection, uniform airflow distribution that reduces hotspots, lightweight and inexpensive production using corrugated metal sheets, and scalability for small-scale applications. Its disadvantages include: fabrication complexity at high iterations that increases costs (up to 20% more expensive), potential dust accumulation in fractal gaps that clogs the flow, and sensitivity to variations in the fractal ratio (FR) where an FR that is too small (<0.5) actually reduces air velocity by up to 15%.

This study developed the Sierpinski Carpet Corrugated Solar Air Heater (SCCA-SAH) to improve tomato drying efficiency, supporting the production of high-value products such as Torakur—date-flavored tomatoes sold for up to Rp60,000/kg [19][20][21]. Experimental methods and CFD simulations were used to analyze the effect of varying fractal ratios (RF = 1, 0.75, 0.6) on heat distribution, efficiency, air velocity, and drying rate [22][23]. This development is expected to reduce losses for Indonesian farmers and encourage agricultural product diversification.

2. SIMULATION METHODS

This chapter provides a comprehensive explanation of the design, including the data collection techniques, location, and timeframe. It also explains the procedures for impartial data processing and assessment to achieve the stated objectives: to determine the distribution of air temperature, air pressure, and air flow velocity within the collector using Computational Fluid Dynamics simulation. This research employed a mixed method, consisting of qualitative and quantitative methods. The quantitative method involved data collection based on research into the decline in tomato selling prices in Indonesia after harvest. The qualitative method utilized ANSYS Fluent software simulations is a Computational Fluid Dynamics (CFD)-based simulations software widely used to analyze fluid flow and heat transfer through three main stages: pre-processing, processing, and post-processing. In the pre-processing stage, the geometry is created in Space Claim with specific dimensions shown in Figure 1(a) and RF variations, then important parts are named and an enclosure is formed to define the flow domain before the simulation proceeds shown in Figure 1(b).

The next step is meshing, which divides the geometric domain into small elements for numerical discretization. Mesh quality greatly affects simulation accuracy, so the size and type of mesh must be adjusted to the complexity of the geometry, where the configuration for each RF variation is shown in Figure 1(c). Numerical calculations were performed using CFD with a k-ε turbulence model and SIMPLE algorithm for pressure-velocity coupling. A three-dimensional steady-state model was used to analyze the effect of RF on heat transfer and flow. The flow regime is assumed to be laminar is selected due to its suitability for internal flow and heat transfer analysis. The light intensity on the upper wall is assumed to be 585 W/m^2. A second-order discretization scheme is applied to the momentum and energy equations to improve numerical accuracy. Convergence criteria are defined based on residual values, with continuity and momentum residuals set to 10^{-4} to ensure physically stable and meaningful solutions in all RF configurations.

The next step is to determine the boundary conditions, including inlet velocity, outlet pressure, temperature, and wall conditions to match the actual conditions. Once all parameters have been determined, the solution process is carried out iteratively until a convergent solution is obtained. Once convergence is achieved, the simulation results are saved and analyzed using the post-processing feature. Post-processing involves analyzing and visualizing the simulation results. This stage is used to obtain an overview of fluid flow, air pressure distribution, air temperature distribution, and air flow velocity, in accordance with the research objectives using the Computational Fluid Dynamics (CFD) method. The dimension, material, and simulation parameter setting can be seen in Tables 1.

3. RESULT AND DISCUSSION

The temperature contour distribution of the three fractal ratio variations shows quite clear differences in heat transfer characteristics. At RF=0.6, it shows that a denser fractal structure increases air mixing, thereby reducing hot spots, but also lowering the maximum temperature increase. This results in a highest temperature peak of 389.7 K with a temperature deviation of 56 K, indicating a higher heating zone and sharper temperature contrast as well as increased local heat transfer but with a less uniform distribution. The differences between these three variations indicate a trade-off between increased heating efficiency and uniformity of heat distribution, so the choice of fractal ratio must be tailored to the system design requirements. Based on the reinterpretation that RF=1 represents the densest fractal distance, the experimental results show a pattern consistent with leading literature studies. An overly dense fractal configuration causes a significant increase in pressure drop and flow resistance, thereby reducing the air mass flow rate and ultimately decreasing heat transfer performance, as reflected in the lowest outlet temperature showing a lower temperature deviation of 54.9 K, indicating a more uniform thermal

distribution, but very little heat transferred. These findings are consistent with the principle in thermal engineering that states that optimization of heat sink geometry must balance between increasing surface area and pressure loss [13].

Figure 2 shows the grid indenpendency for simulation to ensure stability. The results indicate that the air outlet temperature generally increases as the number of cells rises, showing improved resolution of heat transfer with finer discretization. A significant increase is observed when the cell number is raised from 5,000 to 18,000, suggesting that coarse meshes tend to underpredict the outlet temperature. Beyond this range, the temperature variation becomes smaller, indicating that the solution starts to converge. The case with 7,000 cells shows a temperature comparable to higher cell counts, implying that this mesh density already provides a reasonable balance between accuracy and computational cost.

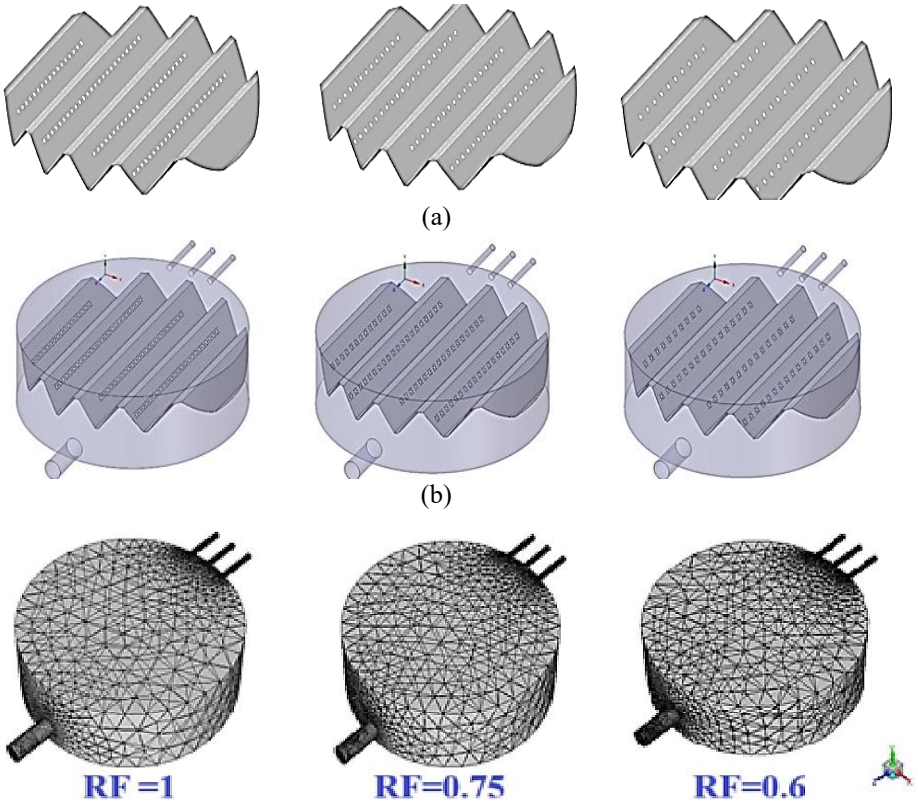

Figure 1. (a) Corrugated Sierpinski Carpet Model, (b) Solar Collector Model, (c) Meshing

Table 1. Dimension, Material, and Simulation Parameter Setting.

Parameter	Settings
Dimension	0,975 mm
Modelling	3D
Material	Aluminum
Boundary Condition	
Inet:	Velocity inlet: 0,5 m/s
Outlet:	Pressure outlet
Top Wall	Heat Flux 585 w/m^2
Bottom and Cover Wall	Adiabatic
Algorithm	SIMPLE
Residual	10-e4
Energy	ON
Temperature inlet	300K
Discretization	First Order

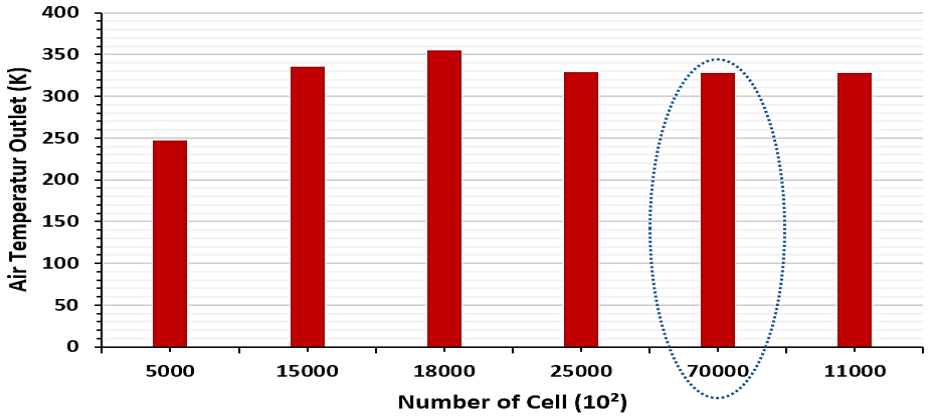

Figure 2. Grid Independency

3.1 Temperatur Distribution

Figure 3 shows the temperature distribution, it shows three distinct behaviors that reflect how the fractal absorber geometry reshapes the heat pickup along the dryer. The RF = 1 curve (blue, triangles) showing a sharp temperature increase of about 34 K in the first third of the channel length, starts cooler near the inlet 300 K, then exhibits a sudden jump around the first third of the channel and remains at a higher plate 334K until 336 K downstream a signature of strong local heat accumulation caused by dense obstacles that trap air and create recirculation zones with long residence times. The RF = 0.75 trace shows in red color, results in an output temperature that is 10-15% lower in the range of 320-330 K and a decrease in efficiency of around 15-15.5%, which indicates less than optimal thermal interaction due to excessively smooth flow. The RF = 0.6 series. It shows the most even, steadily increasing temperature toward the outlet and reaches comparable or slightly higher outlet temperatures, which suggests that the more open fractal spacing promotes beneficial mixing: enough turbulence to enhance surface-to-air heat exchange without producing severe local hot spots or excessive flow resistance. These trends match the simulation observations that fractal spacing controls the trade-off between maximum heating and uniformity as shown in Figure 4. That the fractal ratio (RF) significantly affects thermal behavior within the channel. The RF = 1 configuration produces higher but locally accumulated temperatures due to increased flow obstruction. RF = 0.75 exhibits strong thermal gradients and non-uniform heating. In contrast, RF = 0.6 provides the most uniform temperature distribution, indicating balanced convection–conduction heat transfer and improved thermal stability.

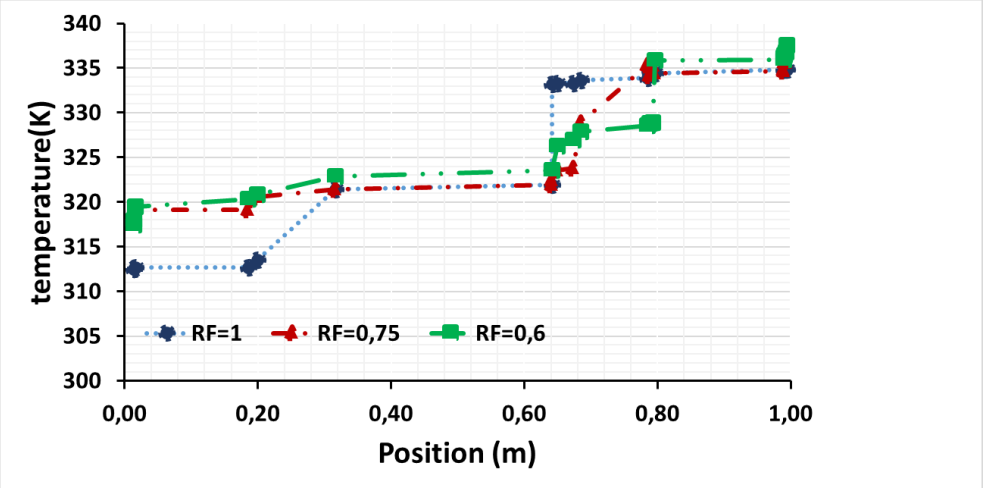

Figure 3. Air Temperature Distribution in Middle Line.

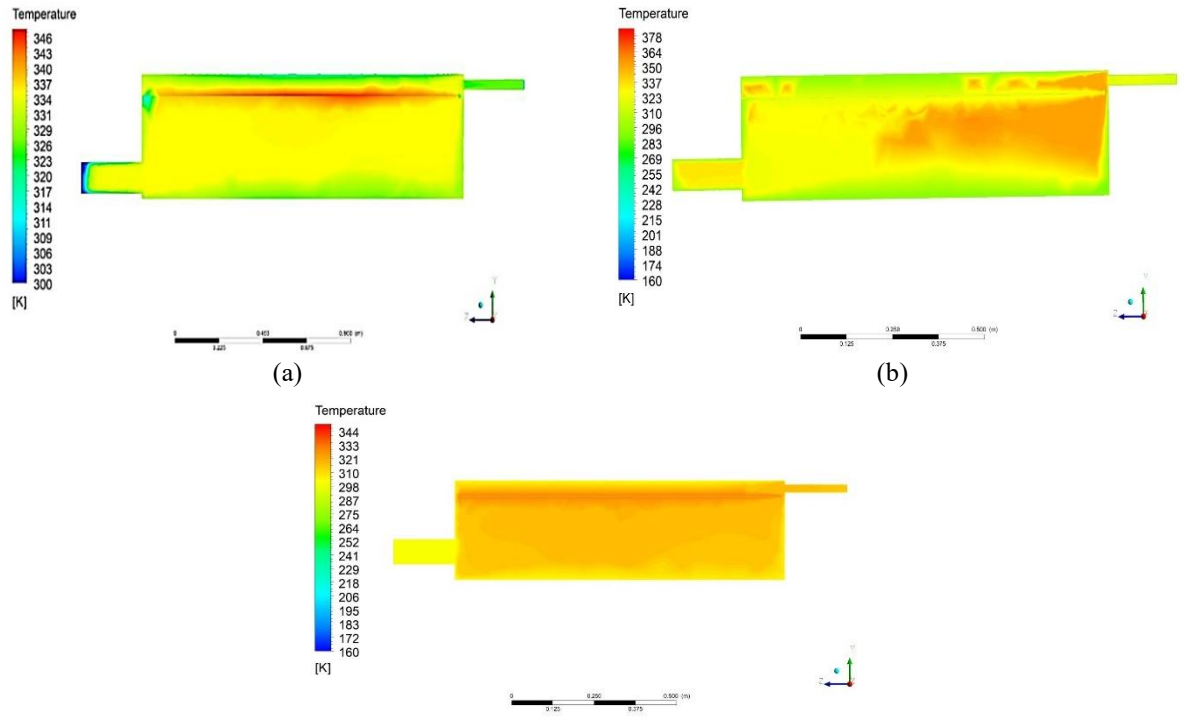

Figure 4. Contour (a) RF=1, (b) RF=0,75, (c) RF=0,6

3.2 Velocity Distribution

The velocity is shown in Figure 5, the chart explains the temperature patterns by revealing how the fractal layout reorganizes the airflow. For RF = 1 the velocity stays modest through the inlet region then accelerates sharply near the downstream constrictions, producing the large peaks seen at the far right; this acceleration follows flow through narrow passages created by dense fractal elements and explains why temperature jumps occur where the air is rapidly compressed and heated locally. RF = 0.75 shows a mid-channel velocity rise (around 0.3–0.5 m) and then a decline toward the outlet — a behavior consistent with moderate obstruction that momentarily boosts convective transport but then allows the flow to slow and re-mix, producing steadier, lower peak temperatures. RF = 0.6 begins with a relatively high inlet velocity that drops and smooths out downstream, indicating an initially open inlet that quickly converts momentum into distributed mixing; this pattern sustains continuous convective transfer and yields a gradual, uniform temperature increase. In short, the velocity plots reveal the hydrodynamic mechanisms acceleration, recirculation, residence time by which fractal spacing controls both local heating and overall thermal performance.

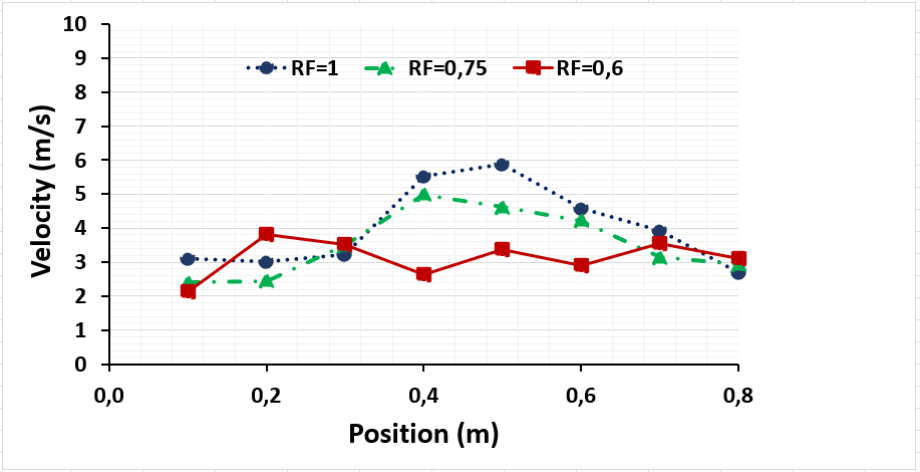

(b)

Figure 5. Air Velocity Distribution in Middle Line.

3.3 Average Temperature and Heat Transfer Efficiency

Table 2. Average Temperature and Heat Transfer Efficiency

Variation	Average Temperature Outlet (K)	Heat Transfer Efficiency (%)
RF=1	328,43	17,14
RF=0,75	326,66	5,46
RF=0,6	328,00	16,72

Based on Table 2, variations in the RF parameter have a noticeable influence on both the average outlet temperature and the heat transfer efficiency as shown below :

$$\Delta T = \frac{Number\ of\ Temperature\ Data}{Total\ Temperature\ Data} \quad (1)$$

$$\eta = \frac{Qactual}{Qmax} \quad (2)$$

At RF = 1, the average outlet temperature reaches 328.43 K, accompanied by the highest heat transfer efficiency of 17.14%. This condition indicates that the system operates near its optimal thermal performance, where the heat exchange process is relatively effective. When the RF value is reduced to 0.75, the average outlet temperature decreases to 326.66 K. More significantly, the heat transfer efficiency drops sharply to 5.46%. This substantial reduction suggests that, under this condition, the heat transfer mechanism becomes less effective, possibly due to unfavorable flow characteristics or reduced turbulence intensity that limits thermal energy exchange. Further reduction of RF to 0.6 results in an increase in the average outlet temperature to 328.00 K, which is comparable to the value observed at RF = 1. The heat transfer efficiency also recovers to 16.72%, approaching the maximum efficiency recorded in this study. This trend indicates that lower RF does not necessarily lead to poorer thermal performance, and that certain RF conditions can enhance heat transfer by improving flow behavior and thermal interaction within the system. Overall, the results demonstrate that the relationship between RF, outlet temperature, and heat transfer efficiency is non-linear. While RF = 1 and RF = 0.6 provide relatively high efficiencies, RF = 0.75 represents a less favorable operating condition. These findings highlight the importance of selecting an appropriate RF value to achieve optimal heat transfer performance.

4. CONCLUSION

1. The variation in fractal ratio (RF) directly shapes how heat is distributed along the channel. A denser configuration (RF = 1) showed a sharp temperature increase of about 30–35 K in the first third of the channel, accompanied by a higher axial temperature gradient compared to other configurations., while more open arrangements (RF = 0.75 and RF = 0.6) allow the air to move more smoothly, resulting in a gentler and more uniform rise in temperature.
2. These heating differences are largely driven by how each fractal layout alters the airflow pattern. When the geometry creates too much resistance, the flow becomes unstable, accelerating and decelerating abruptly, which leads to uneven heating. But when the obstruction is balanced, the airflow stays steady and well-mixed, enabling the thermal energy to be carried more consistently throughout the channel.
3. The heat transfer efficiencies were obtained at RF = 1 and RF = 0.6, with values of 17.14% and 16.72%, respectively, accompanied by relatively high outlet temperatures. In contrast, the RF = 0.75 condition produced a noticeably lower outlet temperature and a substantial decrease in heat transfer efficiency, indicating less effective thermal interaction.
4. The limitation of this simulation lies in the reliance on a first-order approach and intricate parameter settings, which may not completely represent actual operating conditions. Further studies should explore more advanced modeling techniques.

5. ACKNOWLEDGEMENT

This research was funded by the Directorate of Research and Community Service, Direktorat Penelitian dan Pengabdian Masyarakat (DPPM) and supported by the Electronics Engineering Polytechnic Institute of Surabaya, Politeknik Elektronika Negeri Surabaya (PENS).

REFERENCES

[1] Q. Ayun, S. Kurniawan, and W. A. Saputro, "Perkembangan Konversi Lahan Pertanian Di Bagian Negara Agraris," *Vigor J. Ilmu Pertan. Trop. Dan Subtrop.*, vol. 5, no. 2, pp. 38–44, 2020, doi: 10.31002/vigor.v5i2.3040.

[2] T. Pertumbuhan and E. Dalam, "PRESPEKTIF ISLAM (STUDI PADA KABUPATEN TULANG," pp. 205–212, 2024.

[3] S. Sulawesi, "Jurnal Polimesin," vol. 23, no. 3, 2025.

[4] S. F. Purba, A. Yulianti, S. Astana, and R. D. Djaenudin, "The contribution of agricultural crop production towards the economic growth of Indonesia ' s agricultural sector," vol. 34, 2023.

[5] J. Publikasi *et al.*, "Evaluasi Kinerja Sektor Pertanian dalam Kontribusinya terhadap Pendapatan Nasional dengan Pendekatan Metode Produksi," 2025.

[6] R. Sanusi Putri, "Petani Tomat Buang Hasil Panen karena Harga Jeblok dari Rp 4.000 jadi Rp 600 per Kg, Respons Kementan?," Tempo. Accessed: Jul. 02, 2025. [Online]. Available: https://www.tempo.co/ekonomi/petani-tomat-buang-hasil-panen-karena-harga-jeblok-dari-rp-4-000-jadi-rp-600-per-kg-respons-kementan--225861

[7] R. Harmoni, "Harga Anjlok, Petani Di Lembang Biarkan Tomat Membusuk," TV Harmoni. Accessed: Jul. 02, 2025. [Online]. Available: https://tvharmoni.com/2024/08/01/harga-anjlok-petani-di-lembang-biarkan-tomat-membusuk/

[8] Saptana *et al.*, "Competitiveness analysis of fresh tomatoes in Indonesia: Turning comparative advantage into competitive advantage," *PLoS One*, vol. 18, no. 11 November, pp. 1–29, 2023, doi: 10.1371/journal.pone.0294980.

[9] A. Jarman *et al.*, "Postharvest Biology and Technology Postharvest technologies for small-scale farmers in low- and middle-income countries : A call to action," *Postharvest Biol. Technol.*, vol. 206, no. September, p. 112491, 2023, doi: 10.1016/j.postharvbio.2023.112491.

[10] T. Molelekoa, E. M. Karoney, N. Siyoum, and J. K. Gokul, "Quality and Quantity Losses of Tomatoes Grown by Small-Scale Farmers Under Different Production Systems," pp. 1–21, 2025.

[11] S. Soekarno, T. D. Septian, I. Indarto, N. P. Lestari, and R. Nadzirah, "Uji Kinerja Multi Seeds Smart Dryer (MSSD) Pada Kacang Hijau (Vigna Radiata)," *Rona Tek. Pertan.*, vol. 17, no. 2, pp. 94–106, 2024, doi: 10.17969/rtp.v17i2.34808.

[12] et al Barata, L. O. A., "Performance evaluation of a standalone solar PV system: a case study in Kendari, Southeast Sulawesi, Indonesia," *Jural Polimesin*, vol. 23, 2025, doi: http://dx.doi.org/10.30811/jpl.

[13] C. Prasopsuk, K. Sutthivirode, and T. Thongtip, "Performance Enhancement of a Solar Air Heater Equipped with a Tree-like Fractal Cylindrical Pin for Drying Applications: Tests Under Real Climatic Conditions," *Energies*, vol. 18, no. 9, 2025, doi: 10.3390/en18092230.

[14] S. Dryer, U. Flat, and P. A. Plates, "Journal of Engineering," vol. 31, no. 8, pp. 200–226, 2025.

[15] Y. Gao *et al.*, "The Effect of Geometric Parameters on Flow and Heat Transfer Characteristics of a Double-Layer Microchannel Heat Sink for High-Power Diode Laser," 2022.

[16] L. Nguyen and M. Ha, "Heat transfer and flow characteristics in horizontal spiral coils with flat tubes and rectangular ribs : CFD and optimization," *Int. J. Thermofluids*, vol. 26, no. January 2025, p. 101072, 2027, doi: 10.1016/j.ijft.2025.101072.

[17] C. C. By, "Fractal Geometry as an Effective Heat Sink," 2022, doi: 10.5545/sv-jme.2022.28.

[18] J. B. Pascual-Francisco, O. Susarrey-Huerta, L. I. Farfan-Cabrera, and R. Flores-Hernández, "Creep Properties of a Viscoelastic 3D Printed Sierpinski Carpet-Based Fractal," *Fractal Fract.*, vol. 7, no. 8, 2023, doi: 10.3390/fractalfract7080568.

[19] A. D. K. Eko Suharyono, dan Wiharso, "Analisis pendapatan bersih dan kelayakan pengolahan tomat (Solanum lycopersicum) menjadi torakur (tomat rasa kurma) di Kecamatan Bumijawa Kabupaten Tegal," *AGROMEDIA Berk. Ilm. Ilmu-ilmu Pertan.*, vol. 40, no. 2, pp. 68–75, 2022, doi: 10.47728/ag.v40i2.381.

[20] kumparanFOOD, "Foto: Produksi Tomat Rasa Kurma di Kabupten Semarang Saat Bulan Ramadhan," Kumparan Food. Accessed: Jul. 04, 2025. [Online]. Available: https://kumparan.com/kumparanfood/foto-produksi-tomat-rasa-kurma-di-kabupaten-semarang-saat-bulan-ramadan-24ctmUkgFST

[21] N. S. G. Destyana, M. Ferichani, and E. W. Riptanti, "Strategi Pengembangan UKM TORAKUR (Tomat Rasa Kurma) di Kecamatan Bandungan Kabupaten Semarang," *Agrista*, vol. 5, no. 1, pp. 214–224, 2017.

[22] A. Kibishov, G. A. Kilic, N. Rustamov, and N. Genc, "Thermal Analysis of Radiation Heat Transfer of Improved Fractal Solar Collectors," *Appl. Sci.*, vol. 14, no. 23, 2024, doi: 10.3390/app142311155.

[23] M. A. Amraoui and K. Aliane, "Three-dimensional analysis of air flow in a flat plate solar collector," *Period. Polytech. Mech. Eng.*, vol. 62, no. 2, pp. 126–135, 2018, doi: 10.3311/Ppme.11255.

[24] Z. Men and W. Chen, "Heat Transfer Enhancement of Controllable Aspect Ratio Fractal Channel," 2023.